

10 Aug 2016

Designed Extrudate for Additive Manufacturing of Zirconium Diboride by Ceramic On-Demand Extrusion

Devin McMillen

Wenbin Li

Ming-Chuan Leu

Missouri University of Science and Technology, mleu@mst.edu

Greg Hilmas

Missouri University of Science and Technology, ghilmas@mst.edu

et. al. For a complete list of authors, see https://scholarsmine.mst.edu/mec_aereng_facwork/4312

Follow this and additional works at: https://scholarsmine.mst.edu/mec_aereng_facwork



Part of the [Ceramic Materials Commons](#), and the [Manufacturing Commons](#)

Recommended Citation

D. McMillen et al., "Designed Extrudate for Additive Manufacturing of Zirconium Diboride by Ceramic On-Demand Extrusion," *Proceedings of the 27th Annual International Solid Freeform Fabrication Symposium (2016, Austin, TX)*, pp. 929-938, University of Texas at Austin, Aug 2016.

This Article - Conference proceedings is brought to you for free and open access by Scholars' Mine. It has been accepted for inclusion in Mechanical and Aerospace Engineering Faculty Research & Creative Works by an authorized administrator of Scholars' Mine. This work is protected by U. S. Copyright Law. Unauthorized use including reproduction for redistribution requires the permission of the copyright holder. For more information, please contact scholarsmine@mst.edu.

DESIGNED EXTRUDATE FOR ADDITIVE MANUFACTURING OF ZIRCONIUM DIBORIDE BY CERAMIC ON-DEMAND EXTRUSION

Devin McMillen[†], Wenbin Li[†], Ming C. Leu[†], Gregory E. Hilmas[‡], and Jeremy Watts[‡]

[†]Department of Mechanical and Aerospace Engineering,
Missouri University of Science and Technology, Rolla, MO 65409

[‡]Department of Materials Science and Engineering,
Missouri University of Science and Technology, Rolla, MO 65409

Abstract

This work describes a process by which zirconium diboride (ZrB_2) parts may be fabricated using the Ceramic On-Demand Extrusion (CODE) process. An oxide-carbide-nitride system consisting of ceramic powders and pre-ceramic organics, designed to yield ZrB_2 after reaction sintering, has been developed to produce an aqueous-based extrudate for subsequent processing in the CODE system. Pressurelessly sintered test specimens containing 1 wt% PVA binder achieve high relative density $\geq 99\%$. The viscoelastic response of the extrudate was characterized via spindle rheometry with a small sample adapter. Batches with 1 wt% PVA and 0.5 wt% Methocel show strong shear thinning characteristic, under shear rates of $1\text{--}28\text{ s}^{-1}$. XRD and SEM were utilized for microstructural analysis to determine phase development and microstructural morphology.

1. Introduction

Zirconium diboride (ZrB_2) is classified as an ultrahigh temperature ceramic (UHTC), all of which have melting temperatures over 3000°C [1]. This class of material performs well in harsh environments, often exceeding the capabilities of traditional engineering materials. ZrB_2 has a high melting temperature (3245°C), high Young's modulus (526 GPa), high hardness (23 GPa), and low theoretical density (6.09 g/cm^3) [2, 3, 4]. The application of additive manufacturing for UHTCs may provide a cost-effective method for fabrication of complex components for next-generation gas turbines, rocket engines, and hypersonic vehicles [5, 6].

Sintering of non-oxide ceramics is often difficult because of their high melting temperature, due to strong covalent bonds (metallic, ionic, and covalent in the case of ZrB_2). Sintering to high densities is normally achieved through solid-state sintering by pressure-assisted methods, such as hot pressing and hot isostatic pressing. However, these methods limit production to the creation of monolithic geometries, and as such, are not viable for complex geometries often associated with additive manufacturing. Alternative pressureless processing routes have proven equally successful [7, 8]. Pressureless sintering is the promotion of densification without the application of an external pressure upon a body; this is the most common sintering method and often what is referred to when ‘sintering’ a ceramic body [9]. Multiple sintering additives have been found to assist in pressureless sintering of ZrB_2 : 1.7 wt% carbon sintered at 1900°C and 4.5 wt% B_4C sintered at 1850°C resulted in near theoretical density for powder attrition milled with tungsten carbide (WC) media [10].

Reaction sintering is a method in which both chemical reaction and densification occur in a single sintering cycle. Normally a method reserved for production of high purity powders, several reaction paths have been introduced with varying thermodynamic requirements [11, 12, 13]. However, none have been applied to *in situ* fabrication using additive manufacturing (AM). With application of colloidal processing techniques, an extrudate may easily be designed, such that it has the desired rheological properties for deposition, the chemistry for reaction sintering, and a particle size to promote specific phase development [14, 15]. These parameters can be further controlled to promote high relative density without pressure-assisted sintering, such that complex, near net-shape components may be fabricated. Elimination of the machining costs associated with ceramic materials would alone justify *in situ* fabrication. The structural and thermal properties of ZrB_2 are valuable to many industries that would favor a method of production that provides a high degree of compositional control with low machining costs.

Ceramic On-Demand Extrusion (CODE) is an extrusion-based AM process which can successfully fabricate mesoscale artifacts. Using high solids loading (>50 vol%), aqueous, ceramic extrudate, deposition is done at room temperature to build a 3D geometry layer-wise. After deposition, each layer is partially solidified by uniform infrared radiation applied perpendicular to the top face. Concurrently, the built portion is surrounded, flush with the top most layer, by a low molecular weight oil to promote one-dimensional drying. Dynamic drying eliminates a water content gradient in the deposited part, imparts greater stability during the build, and enables the production of fracture and warpage free ceramic parts [16].

Pressureless reaction sintering, applied to CODE, provides a solution to *in situ* fabrication of near net-shape UHTC components with a high degree of microstructural control and minimal post-processing that has not yet been achieved in AM to date. This study is the initial investigation to design an oxide-carbide-nitride extrudate to fabricate highly complex near net-shape components. The goals of this study are as follows: 1) identify viable reaction materials, 2) determine the ratio of additives to promote pressureless sintering to achieve high relative density, 3) maintain nominal purity with high relative density, 4) achieve a high degree of microstructural control, and 5) compare the mechanical properties between pressureless and reaction sintered ZrB_2 parts fabricated by Ceramic On-Demand Extrusion.

2. Experimental Procedure

Commercially available zirconium diboride (ZrB_2 , Grade B, H.C. Starck, Karlsruhe, Baden-Württemberg, Germany) and boron carbide (B_4C , Grade HS, H.C. Starck, Karlsruhe, Baden-Württemberg, Germany) powder were used in this study for pressureless sintering trials to establish a baseline sintering temperature. The reported average particle size was in a range of $1.5\text{-}3.0\text{ }\mu\text{m}$ with a 97% (metal basis) purity for ZrB_2 ; the average particle size of the B_4C powder was $0.8\text{ }\mu\text{m}$, with a surface area of $15\text{-}20\text{ m}^2/\text{g}$, and a B:C ratio of 3.7-3.8.

To prepare an extrudate for *in situ* fabrication of ZrB_2 , zirconia (ZrO_2 ; Inframet Advanced Materials, Manchester, Connecticut, USA), boron nitride (BN; Grade F 15, H.C. Starck, Karlsruhe, Baden-Württemberg, Germany), and graphite (Carbon Black, Cabot, Alpharetta, Georgia, USA) were attrition-milled in methyl ethyl ketone (MEK, Sigma Aldrich, St. Louis, Missouri, USA) at 600 rpm for 2 h; BN had a reported average particle size of $6.0\text{ }\mu\text{m}$ and surface area of $10\text{-}20\text{ m}^2/\text{g}$.

A high molecular weight polyvinyl alcohol (PVA; avg. molecular weight 70,000-100,000, Sigma Aldrich, St. Louis, Missouri, USA) and cold water dispersible hydroxypropyl methylcellulose (Methocel J5MS, DOW, Midland, Michigan, USA) solutions were used as water-soluble binders.

The surface area of as-received powder was measured using nitrogen adsorption analysis according to Brunauer-Emmett-Teller (Nova2000e, Quantachrome Instruments, Boynton Beach, Florida, USA) and the particle size distribution by laser diffraction (S3500, Microtrac, York, Pennsylvania, USA). Sedimentation studies were used to approximate the best concentration of dispersant on a surface area basis, using Darvan C-N (ammonium polymethacrylate; Vanderbilt Minerals, LLC, Norwalk, Virginia, USA) and Dolapix CE 64 (carbonic acid; Zschimmer & Schwarz, Lahnstein, Rhineland-Palatinate, Germany). In the known pH regime for stability, 0.5-2.0 mg/m² dispersant was added to respective 10 mL graduated cylinders; 3 g of powder was added to each cylinder; 10 mL pH adjusted solvent was added; each cylinder was covered using paraffin film, agitated, then ultrasonicated for 600 s before being left stationary for sedimentation. The pH value was measured using a pH meter (HI 2210, Hannah Instruments, Woonsocket, Rhode Island, USA) and adjusted dropwise using an ammonium hydroxide solution (NH₄OH, 30% NH₃ basis, Sigma Aldrich, St. Louis, Missouri, USA).

2.1 Pressureless Sintering

A ZrB₂ composition with 4 wt% B₄C additive was used for pressureless sintering studies. These powders were attrition-milled in a polymer-lined jar using cobalt-bonded tungsten carbide (WC) media at 600 rpm for 2 h in acetone or MEK. After milling, the powder was retrieved via rotary evaporation (Rotovapor R-124, Buechi, Flawil, St. Gallen, Switzerland). The powder was then crushed using a diamonite mortar and pestle and passed through a sieve stack: 250 µm / 60 mesh; 150 µm / 100 mesh; 106 µm / 140 mesh; and 90 µm / 170 mesh. Collected powder was uniaxially pressed into pellets for a sintering study. Two samples, each of five pellets, were made using a laboratory benchtop press (model 3851-O, Carver, Wabash, Indiana, USA); one set with and the other without PVA-binder. Due to incompatibility between PVA and MEK, batches that included binder were milled in acetone. After the doped ZrB₂ powder was retrieved, PVA binder was introduced as a 10 wt% solution, and the mixture was milled in a HDPE wide-mouth bottle with WC media for 2 h to homogenize. Solvent was removed by boiling the slurry under a high (700-1200) rpm stir until dry. For each pellet, 1.5 g of powder was loaded into a 12.7 mm die and pressed for 60 s at 70.3 MPa; between compaction, the die was cleaned with acetone and lubricated with stearic acid.

The samples were sintered individually; a 6.35 cm dia. x 5.33 cm tall cylindrical graphite crucible was lined with flexible graphite foil (GRAFOIL, GrafTech Intl., Parma, Ohio, USA) and coated with an aerosol boron nitride lubricant (BN SP-2018, Materion, Buffalo, New York, USA) for sintering. Once dry, the crucible was loaded and topped with a permeable graphite foil lid. The sintering schedule was carried out in a resistance-heated, graphite, bottom-loading furnace (model 1000-4360-FP30, Thermal Technology Inc., Santa Rosa, CA, USA). The furnace was ramped from room temperature to 700°C at 10°C/min in flowing argon. Once at temperature, the furnace was held for 0.5 h before ramping to 1450°C at 10°C/min. A partial vacuum (~160-120 millitorr) was

pulled and the temperature held for 1 h. Afterward, the furnace was ramped to 1600°C at 10°C/min and held for 1 h. During these high temperature isothermal holds, the mild vacuum was monitored; an increase in pressure indicates volatilization of material or the reaction is occurring. A manual hold, not exceeding an additional 15 min, was performed to allow the vacuum to decrease as much as possible before proceeding. The final ramp from 1600°C to 1900°C at 30°C/min occurred under flowing argon, then dwelled for 2h to sinter, and cooled to 50°C at a rate of 30°C/min.

Relative density of each sample was determined using the Archimedes' method with water as the immersion medium. All pellets were weighed to obtain their dry mass, D , put in individual beakers of distilled water, and brought to a boil. Then the beakers were transferred to a vacuum chamber, where they were infiltrated for 24 h. The vacuum was checked and re-pulled at 10 h to ensure integrity. After the saturated weight, M , and suspended weight, S , were measured and the bulk density was calculated according to Equation 1 [17]:

$$B = \frac{D}{M-S} \quad (1)$$

Percent relative density is then determined by dividing the bulk density, B , by theoretical density. The value of the theoretical density of a mixed powder is determined by a rule of mixtures calculation.

Specimens achieving higher than 98% theoretical density were then mounted to polish the face of the pellet to a 0.25 μm finish using successively finer diamond abrasives. The specimens were chemically etched in a 1:1 KOH solution at 200°C for 30 s; their microstructures were analyzed using scanning electron microscopy (SEM; field emission S-4700, Hitachi, Schaumburg, Illinois, USA). An average grain size was measured using ImageJ, which is an open source imaging software.

2.2 Reaction Sintering

The sequence of reactions in Table 1 was the assumed route of reaction for *in situ* reaction sintering. Reactions (2) - (5) represent sequential and concurrent reactions, while reaction (1) is the intended overall reaction. The Gibbs free energy (ΔG) values can be calculated using: $\Delta G = \Delta G^\circ + RT \ln K_p$, where ΔG° is the change in standard state Gibbs free energy, R is the ideal gas constant, T is the temperature, and K_p is a reaction constant.

Table 1: Intended reaction path and Gibbs free energy for each reaction step.

Reaction	ΔG (kJ)
(1) $\text{ZrO}_2 + 2\text{BN} + 2\text{C} \rightarrow \text{ZrB}_2 + 2\text{CO} + \text{N}_2$	$\Delta G = 1055.6 - 0.761T$ ($\Delta G < 0$, $T > 1115^\circ\text{C}$)
(2) $4\text{BN} + \text{C} \rightarrow \text{B}_4\text{C} + 2\text{N}_2$	$\Delta G = 941.0 - 0.487T$ ($\Delta G < 0$, $T > 1659^\circ\text{C}$)
(3) $2\text{ZrO}_2 + \text{B}_4\text{C} + 3\text{C} \rightarrow 2\text{ZrB}_2 + 4\text{CO}$	$\Delta G = 1170.3 - 1.002T$ ($\Delta G < 0$, $T > 895^\circ\text{C}$)
(4) $\text{ZrO}_2 + 3\text{C} \rightarrow \text{ZrC} + 2\text{CO}$	$\Delta G = 679.8 - 0.503T$ ($\Delta G < 0$, $T > 1078^\circ\text{C}$)
(5) $\text{ZrC} + 2\text{BN} \rightarrow \text{ZrB}_2 + \text{N}_2 + \text{C}$	$\Delta G = 375.9 - 0.241T$ ($\Delta G < 0$, $T > 1287^\circ\text{C}$)

The reactants for reaction (1) were verified for nonstandard states, under flowing argon and partial vacuum, using thermodynamic software, FactSage 7.0. A composition was batched according to the molar ratios of reaction (1) and mixed with WC media in a mill jar for 1 h in MEK. The solvent was removed via rotary evaporation and the powder uniaxially pressed according to the same procedure as the pressureless sintering study. These specimens were reaction sintered using the same rates and isothermal holds as the pressureless sintering study; this is to verify the times and temperatures for reaction. After reaction, the crystalline phases were identified using powder X-ray diffraction (XRD; PANalytical X'pert Phillips, Eindhoven, The Netherlands).

2.3 Extrudate Batching

Formulation of 55 vol% 10 mL test batches were done by mixing milled $\text{ZrB}_2 + 4 \text{ wt\% B}_4\text{C}$ powders in 50 mL beakers using a flat stainless steel spatula. After achieving a smooth mixture, a binder solution was introduced, of which two types were used for the formulation of extrudate: PVA and Methocel. A baseline concentration of 1 wt% was used for PVA, while Methocel concentrations were 0.5 and 0.25 wt%. Rheometry was employed to measure the viscoelastic response of each extrudate batch.

Due to a lack of applied pressure during fabrication with CODE, in comparison to uniaxial pressing, sintering additives must be included and their effect on the viscoelastic response must also be measured. For deposition of a thick-walled specimen of mesoscale architecture, a shear-thinning rheology is favorable, such that the extrudate behaves like a solid after deposition.

2.4 Rheometry

A digital rheometer (DV-III, Brookfield AMETEK, Inc., Middleboro, Massachusetts, USA) was used for all viscosity measurements, using a small sample adapter and a number 28 spindle. With these peripherals, the possible viscosity range is 200-5,000,000 cP and the possible shear rate range is $0\text{-}56 \text{ s}^{-1}$. The chamber is loaded with 10 mL of extrudate, then the spindle is attached and inserted into the extrudate. Once the rheometer is loaded with a sample, a high shear history is put on the sample by running at 100 RPM for 300 s. Afterward, a viscosity reading is taken every 10 s for 180 s, then the torque is recorded. This is repeated three times for each respective RPM; the RPM is stepped 100, 75, 50, 25, and 5 to provide a range of shear stress.

3. Results and Discussion

Two powders were investigated to confirm the efficacy of pressureless sintering a UHTC: $\text{ZrB}_2 + 4 \text{ wt\% B}_4\text{C}$ and $\text{ZrB}_2 + 4 \text{ wt\% B}_4\text{C} + \text{PVA binder}$. Compact specimens of each composition were pressed at 70.3 MPa and sintered at 1900°C. Pellets pressed without a binder sintered to ~70% of theoretical density, while specimens containing PVA binder sintered to near theoretical density ($\geq 99\%$), due to increased green density.

Powders used for dispersion were characterized with surface area and particle size analysis, the results of which are listed in Table 2. For colloidal processing, by definition, some dimension of the powders used must be below one micrometer ($< 1 \mu\text{m}$). Stability can be achieved using acrylic surfactants to electrosterically disperse particles in suspension, which is greatly affected by particle size distribution, particle geometry, and surface area.

Dispersions with Darvan C-N and Dolapix CE 64 all suggest 0.5 wt% Darvan C-N to be most effective at dispersing submicron ZrB_2 powder in an alkaline $\text{pH} \approx 10$ suspension. Dispersions were checked every 1800 s and most of these rapidly sedimented, leaving a clear or nearly transparent supernatant fluid after 3600 s. The accuracy of this test is in question without zeta potential measurements to verify the dispersion stability; however, it is known that the isoelectric point of ZrB_2 is $\text{pH} \sim 4.5$ according to studies done by Leo et.al. [14], and that an alkaline $\text{pH} > 8.0$ will provide maximum stability.

Table 2: Measured physical properties of powders.

Material	Surface Area (m^2/g)	Average Particle Size, d_{50} (μm)
Boron Carbide (B_4C)	16.653	0.82
Boron Nitride (BN)	9.931	-
Graphite (C)	30.172	-
Zirconia (ZrO_2)	15.467	0.53
Zirconium Diboride (ZrB_2)	1.849	2.58

Rheometry of the high solids loading test batches with PVA and Methocel binders shows a strong non-Newtonian relationship for batches with 1 wt% PVA and 0.5 wt% Methocel (Figure 1). The downward trend of decreasing viscosity with increasing shear rates is the hallmark of non-Newtonian response, i.e. shear thinning. One batch of 1 wt% PVA was tested 24 hr after batching, to determine the effect of sedimentation and current extrudate shelf-life. At the lowest shear rates, the drag on the spring-spindle assembly reached the maximum torque; similar behavior is seen with low concentrations of Methocel. This response is due to high shear stress from friction between the sediment, in the case of the PVA solution, and due to low concentrations of Methocel, which would otherwise act as a plastic barrier between particles. Higher concentrations of binder exceeded the maximum viscosity of the rheometer, while lower concentrations did not provide consistent data, trial to trial, across the entire shear stress range. An alternative method to measure the viscoelastic response of high solids loading suspension would be favorable to fully characterize viscoelastic response with a more representative range of additive concentrations.

Microstructural analysis was done to measure the average grain size and verify the sintering schedule of pressurelessly sintered $\text{ZrB}_2 + 4 \text{ wt\% B}_4\text{C}$. As shown in Figure 2, there is no intergranular or intragranular porosity, which verifies the sintering time and temperature to achieve high relative density. In the high magnification image (a), it is possible to see some voids, but this is due to polishing and the caustic nature of the KOH etchant, not a product of sintering. A grain

size analysis was done using ImageJ to measure the average grain area and estimate an equivalent circular diameter. Using this method, the approximate grain diameter of the specimens sintered at 1900°C is 10.56 μm , based on a count of 797 grains. This included only the grey phase, in Figure 2, which is ZrB_2 , while the black phase is B_4C .

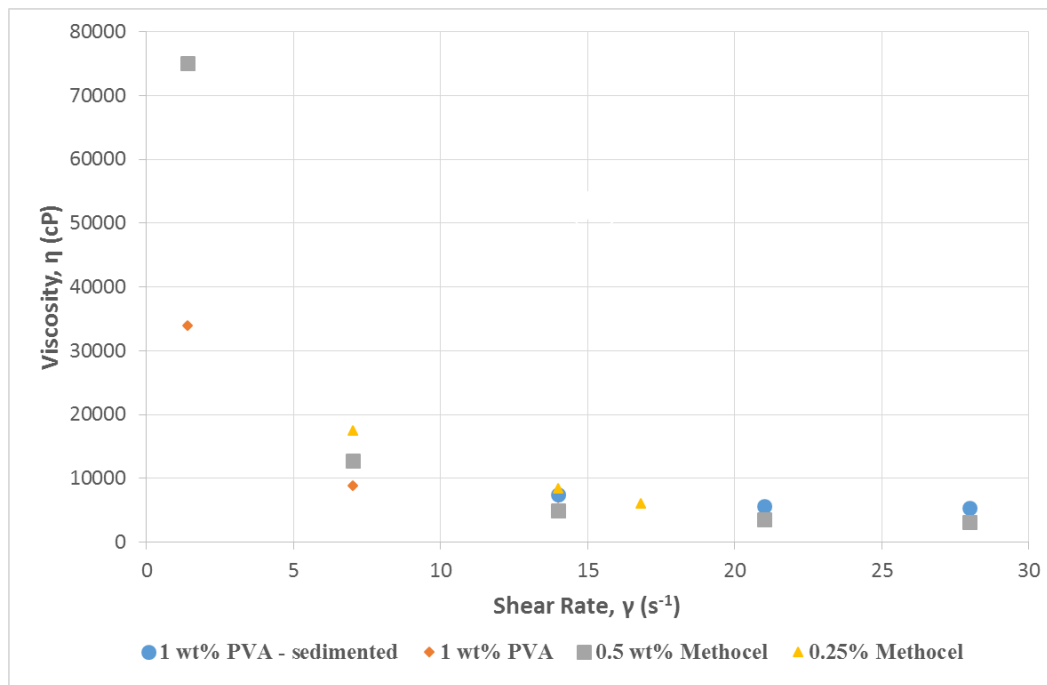


Figure 1: Comparison of PVA and Methocel binders in high solids loading batches.

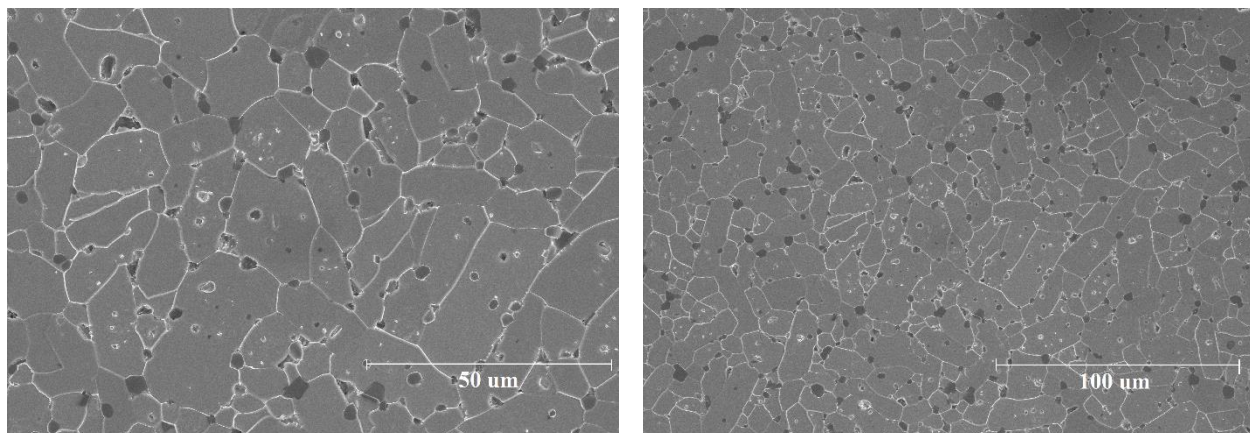


Figure 2: Microstructure of pressurelessly sintered ZrB_2 ; (a) high magnification showing no inter- or intragranular porosity; (b) low magnification, showing grain development and pinning.

A reaction to yield ZrB_2 is often the decomposition of a boron species (borothermal) or carbon species (carbothermal) with a zirconium source. The oxide-carbide-nitride system proposed is a hybrid boro/carbothermal reduction. This multi-step reaction (Table 1) was verified by thermochemical software, however the path may be effected or hindered by particle size, the isothermal holds during sintering, and partial vacuum steps during sintering. For this reason, powder XRD analysis of crushed samples was used to identify the product, revealing that the predominant crystallographic phase of the powder sample was zirconium diboride (Figure 3a). Residual phases from incomplete reaction would present themselves as intermediate intensity peaks, such that peaks in Figure 3b rows 3-5 would be present in rows 1. However, this is not the case, as the peaks of the scanned sample, Figure 3a and 3b row 1, correspond to the chemical tag of zirconium diboride (Figure 3B row 2). None of the major peaks of the reactants, Figure 3b rows 3-5, present themselves in Figure 3a or 3b row 1, confirming the formation of single phase crystalline zirconium diboride.

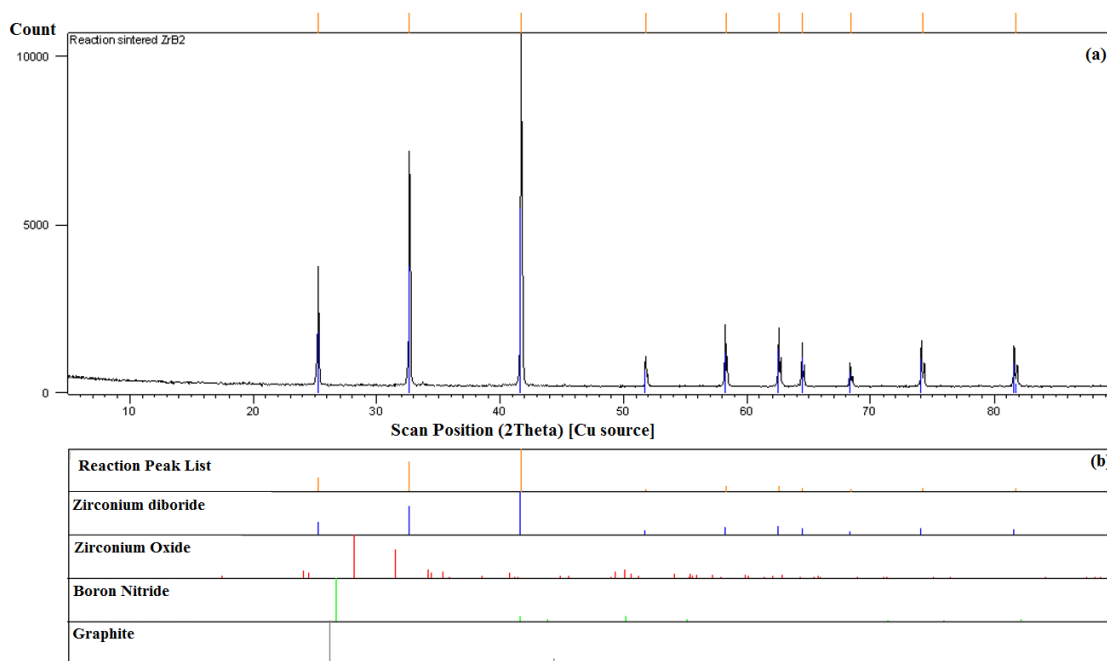


Figure 3: XRD Micrograph of predominant phase of reaction sintered ZrB_2 .

4. Conclusion and Future Work

Our goals stated within the scope of this study, 1) identify viable reaction materials, and 2) determine the ratio of additives to promote pressureless sintering to achieve high relative density, have been achieved. A relative density $\geq 99\%$ was achieved by pressurelessly sintering milled $\text{ZrB}_2 + 4 \text{ wt\% B}_4\text{C}$ at 1900°C , and a successful oxide-carbide-nitride system was established to yield ZrB_2 with an average grain size of $10.56 \mu\text{m}$. Two aqueous binders were presented as options for developing an extrudate for reaction sintering; both PVA and Methocel show a high degree of shear thinning at low weight percentage, which is ideal for CODE deposition.

Further study is necessary to fully characterize the extrudate via rheometry; the storage and loss moduli are of particular interest for non-Newtonian extrudate. Having confirmed a chemistry for reaction sintering, further development is necessary to achieve high relative density. Once achieved, green ceramic parts will be fabricated using CODE for mechanical testing and microstructural analysis.

Acknowledgments

The authors gratefully acknowledge the financial support by the National Energy Technology Laboratory of the Department of Energy under the contract #DE-FE0012272, and by the Intelligent Systems Center at the Missouri University of Science and Technology.

References

- [1] X. Zhang, J. Han, and Z. Wang, *ZrB₂ and ZrB₂-based Ceramics*, Lexington, KY, LAP Lambert Academic Publishing (2014).
- [2] W.G. Fahrenholtz and G.E. Hilmas, "Refractory Diborides of Zirconium and Hafnium," *J. Am. Ceram. Soc.*, 90 [5] 1347-1363 (2007).
- [3] N.L. Okamoto, M. Kusakari, K. Tanaka, H. Inui, and S. Otani, "Anisotropic Elastic Constants and Thermal Expansivities in Monocrystal CrB₂, TiB₂, and ZrB₂," *Acta Materialia*, 58 (2010) 76-84.
- [4] A.L. Chamberlain, W.G. Fahrenholtz, and G.E. Hilmas, "Pressureless Sintering of Zirconium Diboride," *J. Am. Ceram. Soc.*, 89 [2] 450-456 (2006).
- [5] A. Li, A.S. Thornton, B. Deuser, J. Watts, M.C. Leu, G.E. Hilmas, and R.G. Landers, "Freeze-Form Extrusion Fabrication of Functionally Graded Material Composites using Zirconium Carbide and Tungsten," *Solid Free. Fabr. Symp.*, Austin, TX, USA (2012).
- [6] T. Huang, G.E. Hilmas, and W.G. Fahrenholtz, "Dispersion of Zirconium Diboride in an Aqueous, High-Solids Paste," *Int. J. Appl. Ceram. Technol.*, 4 [5] 470-479 (2007).
- [7] S.C. Zhang, G.E. Hilmas, and W.G. Fahrenholtz, "Pressureless Densification of Zirconium Diboride with Boron Carbide Additions," *J. Am. Ceram. Soc.*, 89 [5] 1544-50 (2006).
- [8] W.G. Fahrenholtz, G.E. Hilmas, S.C. Zhang, and S. Zhu, "Pressureless Sintering of Zirconium Diboride: Particle Size and Additive Effects," *J. Am. Ceram. Soc.*, 91 [5] 1398-1404 (2008).
- [9] M.N. Rahaman, *Ceramic Processing and Sintering*, Boca Raton, FL, CRC Press (2003).

- [10] S. Zhu, W. G. Fahrenholtz, G. E. Hilmas, and S.C. Zhang, "Pressureless Sintering of Zirconium Diboride using Boron Carbide and Carbon Additions," *J. Am. Ceram. Soc.*, 90 [11], 3660–63 (2007).
- [11] C. Yan, R. Liu, C. Zhang, Y. Cao, and X. Long, "Synthesis of ZrB₂ Powders from ZrO₂, BN, and C," *J. Am. Ceram. Soc.*, 99 [1] 16-19 (2016).
- [12] L. Zoli, A.L. Costa, and D. Sciti, "Synthesis of Nanosized Zirconium Diboride Powder via Oxide-borohydride Solid-State Reaction," *Scripta Materialia*, 109 (2015) 100-103.
- [13] C. Yan, R. Liu, C. Zhang, Y. Cao, and Z. Long, "Synthesis of ZrB₂ Powders from ZrO₂, BN, and C," *J. Am. Ceram. Soc.*, 99 [1] 16-19 (2016).
- [14] S. Leo, C. Tallon, and G.V. Franks, "Aqueous and Nonaqueous Colloidal Processing of Difficult-to-Densify Ceramics: Suspension Rheology and Particle Packing," *J. Am. Ceram. Soc.*, 97 [12] 3807-17 (2014).
- [15] J.A. Lewis, "Colloidal Processing of Ceramics," *J. Am. Ceram. Soc.*, 83 [10] 2341-59 (2000).
- [16] A. Ghazanfari, W. Li, M.C. Leu, G.E. Hilmas, A novel extrusion-based additive manufacturing process for ceramic parts, in: D. Bourell, J. Beaman, R. Crawford, S. Fish, H. Marcus, C. Seepersad (Eds.), *Solid Free. Fabr. Symp.*, Austin, TX, USA, 2016.
- [17] ASTM, *Standard Test Method for Water Absorption, Bulk Density, Apparent Porosity, and Apparent Specific Gravity of Fired Whiteware Products, Ceramic Tiles, and Glass Tiles*. No. ASTM C373- 14A (2014).